Scramjet Nozzles

T Cain
Gas Dynamics Ltd.,
2 Clockhouse Road, Farnborough, GU14 7QY
Hampshire, UK

tcain@gasdynamics.co.uk

ABSTRACT

The lecture is given in four parts, each being a step in the process of nozzle design, and within each part the methods and techniques preferred by the lecturer are presented. We begin with a reminder concerning control volumes and the separation of aerodynamic and propulsive forces and moments. Then it is demonstrated how an appropriate control volume can help define the propulsive force vector that maximises cruise efficiency. The third part recounts Rao's method for maximising thrust when nozzle length is restricted and the final part introduces a new, simpler, Method of Characteristics (MOC) for non-equilibrium flows.

1 INTRODUCTION

Often the lecture on nozzles is given by the same person that spoke on intakes, as is the case in this series. The topics have much in common, they are both concerned with the change in stream thrust that results when the area of the stream is altered. A good intake minimises the loss in stream thrust when the area is contracted, a good nozzle maximises the gain in stream thrust when the area is expanded. The ideal in both cases being limited to the change in stream thrust for an isentropic expansion/contraction between uniform, parallel, inlet/outlets.

The lecture on intakes focussed on applied design using retired aircraft and missiles as examples, but a reference was made to the relevant section of the Handbook of Supersonic Aerodynamics [1] for those seeking an introduction to the art. The same section of the handbook and the same recommendation applies to this nozzle problem but I would add to that the study by Vahl and Weidner [2]. Ideally those freely available sources would allow us to advance to an exploration of the intricacies of previous designs, but unfortunately there are no scramjet nozzles to examine. Almost all are simply conceptual designs and most of these seem to assume that a nozzle is a flat plate that links the end of the combustor to the trailing edge of the aircraft. There are good engineering reasons for keeping nozzle geometry simple: variable geometry may be required; and the surface will be subjected to high heat loads restricting the choice of suitable materials. Material choice has direct implications for structural mass and imposes indirect constraints through restricted construction and fabrication techniques. However rather than abandon the notion of a contour altogether, a better response to these difficulties is to approximate a continuous contour by a series of flat plates as investigated by Vahl and Weidner [2].

When net thrust is a small fraction of gross thrust, great care must be taken with the exhaust in order to generate *any* net thrust. So the most plausible reason for the popularity of crude nozzles and the apparent lack of interest in performance, is that the overwhelming majority of scramjet engines and scramjet powered aircraft concepts were never intended to fly. Preparation for a flight test forces attention to the essentials in a way that academic discipline does not, but the published output from programmes such as NASP and HYPER-X that have benefited from this focus is not yet sufficient to use as a case study. The short supply of background material means no time/space is required to describe nozzle types leaving more available for describing the techniques and tools required for nozzle design. Four steps in the process of scramjet nozzle definition are covered:

Report Documentation Page

Form Approved
OMB No. 0704-0188

1. REPORT DATE	2. REPORT TYPE	3. DATES COVERED
SEP 2010	**N/A**	**-**

4. TITLE AND SUBTITLE	5a. CONTRACT NUMBER
Scramjet Nozzles	5b. GRANT NUMBER
	5c. PROGRAM ELEMENT NUMBER
6. AUTHOR(S)	5d. PROJECT NUMBER
	5e. TASK NUMBER
	5f. WORK UNIT NUMBER
7. PERFORMING ORGANIZATION NAME(S) AND ADDRESS(ES) **Gas Dynamics Ltd., 2 Clockhouse Road, Farnborough, GU14 7QY Hampshire, UK**	8. PERFORMING ORGANIZATION REPORT NUMBER
9. SPONSORING/MONITORING AGENCY NAME(S) AND ADDRESS(ES)	10. SPONSOR/MONITOR'S ACRONYM(S)
	11. SPONSOR/MONITOR'S REPORT NUMBER(S)

12. DISTRIBUTION/AVAILABILITY STATEMENT
Approved for public release, distribution unlimited

13. SUPPLEMENTARY NOTES
See also ADA564620. High Speed Propulsion: Engine Design - Integration and Thermal Management (Propulsion a vitesse elevee : Conception du moteur - integration et gestion thermique)

14. ABSTRACT
The lecture is given in four parts, each being a step in the process of nozzle design, and within each part the methods and techniques preferred by the lecturer are presented. We begin with a reminder concerning control volumes and the separation of aerodynamic and propulsive forces and moments. Then it is demonstrated how an appropriate control volume can help define the propulsive force vector that maximises cruise efficiency. The third part recounts Rao's method for maximising thrust when nozzle length is restricted and the final part introduces a new, simpler, Method of Characteristics (MOC) for non-equilibrium flows.

15. SUBJECT TERMS

16. SECURITY CLASSIFICATION OF:			17. LIMITATION OF ABSTRACT	18. NUMBER OF PAGES	19a. NAME OF RESPONSIBLE PERSON
a. REPORT	b. ABSTRACT	c. THIS PAGE			
unclassified	**unclassified**	**unclassified**	**SAR**	**16**	

1. Control volumes and the separation of aerodynamic and propulsive forces and moments;
2. Determining propulsive forces for maximum cruise efficiency;
3. Optimised thrust for length constrained nozzles;
4. Method of characteristics (MOC) in non-equilibrium flows.

2 CONTROL VOLUMES

2.1 Force accounting

Students of thermodynamics quickly learn how easy it is to make a mistake in the calculation of the net force acting on system if they fail to define their control volume (CV). When it comes to propulsion/airframe integration (PAI) we probably need to be reminded of this useful concept. The minimal interaction between engine and airframe in most subsonic aircraft results in little error if an engine is selected on the basis that its thrust matches the airframe drag. With that aeronautical background it is easy to forget that these are two components of the same system, and that the balance of forces in cruise does not have to be viewed as lift equals weight and thrust equals drag. However if driven to separate the propulsive and aerodynamic forces, particular care is required when they are closely coupled. The discipline of PAI appears to have grown in response to this problem. There is much discussion regarding the virtues of different force accounting methods but not one I have read reminds the reader that the problem is one he has encountered before and its solution is to draw a CV. There are two simple rules to follow when drawing a surface that defines the CV:

a) Ensure the surface is complete (without gaps) and that no part of the aircraft penetrates the surface of the CV unless the forces and moments acting on that part are known at the CV surface;

b) Draw the CV surface where pressures and momentum fluxes are known.

The art/skill of force accounting is drawing a CV where the pressures and momentum fluxes are easiest to calculate. Integration of pressures and momentum fluxes over the CV surface will normally result in non-zero net forces and moments. In cruise, the net force will equal the weight of the aircraft, and the net moment about the aircraft's centre of gravity will be zero. A finite horizontal force tells you the aircraft will accelerate (or decelerate) and finite moments tell you that it will pitch or yaw. Levels of acceleration (linear or rotational) can be calculated this way, but that is only an approximation since the flow within the control volume is treated as quasi steady. In aeronautical terms that is equivalent to assuming the dynamic derivatives are zero.

2.2 Application

Figure 1: Control volumes for two airbreathing missiles, the blue control surfaces enclose the entire missile the red lines mark regions delegated to propulsion

To reinforce the idea expressed above, consider the two air breathing missiles sketched in figure 1. The one on the left is something like the MBDA Meteor, being cylindrical with two ventral intakes. The blue line indicates a control surface that is identical with the missile surface everywhere except where the CV surface crosses the entrance to the intakes and the nozzle exit plane. These regions are marked with a second line in red. We could arbitrarily declare these surfaces as propulsion, then integrate pressure and

momentum fluxes over them to find the propulsive forces and the moments relative to some reference point. Note that the momentum flux crossing the intake entrance plane will, in general, include a vertical component and the engine (as defined) will produce a normal force. The momentum flux and pressures will also result in pitching moments. Some legacy trajectory codes might not be able to deal with anything other than axial forces from engines, reflecting the class of problem they were written to model. A modern code should expect a vector of forces and moments to be generated by the propulsion routine.

The missile on the right is something like the Boeing X-51. The control surface defined in blue is what one might adopt in order to model its performance. Applying CFD to calculate surface pressures everywhere including the internal walls upstream of the isolator entrance, where the control surface is also marked in red. The CFD solution would provide a non uniform flow at the entrance to the isolator, but by integrating over it to find the axial stream thrust, mass flow, and stream power (enthlapy and kinetic energy) one could find equivalent one dimensional conditions for input to a dual mode scramjet model. The engine model would provide the conditions at the nozzle exit plane, the other part of the control surface marked in red. The integration at the isolator entrance would in general result in a normal force, and pitching moments (and side force and yawing moments given side slip) and these would contribute to the total propulsion forces and moments.

These two examples may appear trivial, and they are, as is every other question relating to force accounting. The problem is made simple by the control volume approach from classical thermodynamics, one just needs to apply the method without bending the rules. There is an infinite choice of control volumes in any application, but only those on which pressure and momentum fluxes are known on every part of the three dimensional surface that defines them, are useful. A properly chosen control volume not only simplifies the analysis, but can guide the design process itself.

3 MAXIMISING CRUISE EFFICIENCY

3.1 The ideal supersonic wake

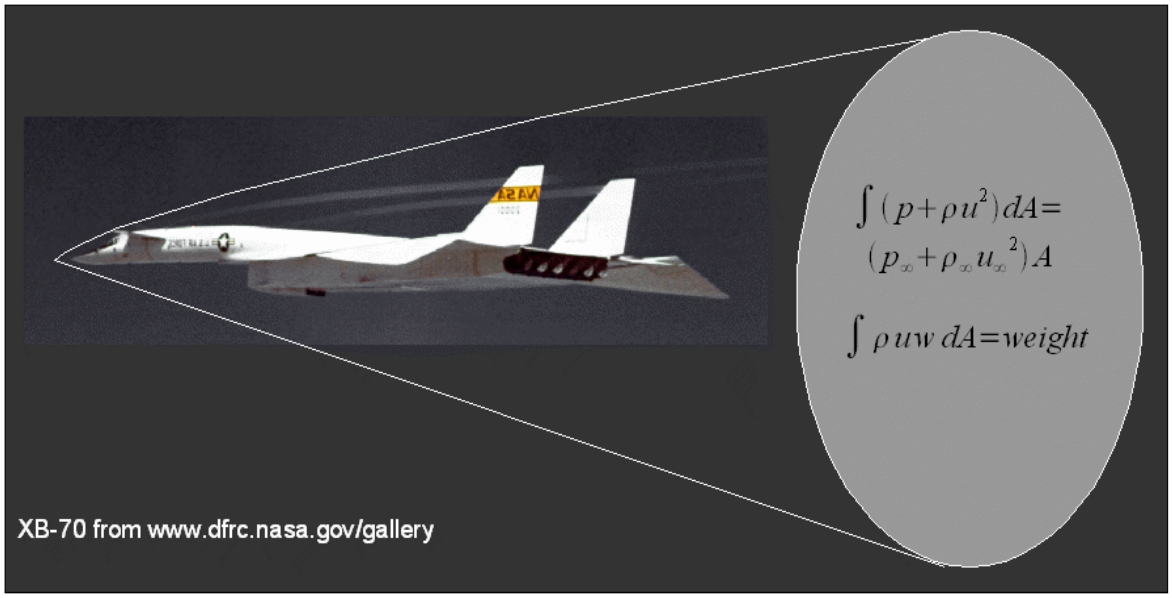

Figure 2 A control volume defined by the intersection of the bow shock and a vertical plane normal to the horizontal flight velocity vector.

Consider the control volume bounded by the envelope of the shock wave emanating from the nose tip of the XB-70, and the outflow plane that is normal the flight direction with a perimeter defined by its

intersection with the shock wave envelope. For the aircraft to be in steady level flight, the downward momentum flux across this outflow plane must equal the aircraft weight (figure 2). On the other hand there must be no change in stream thrust in the flight direction or else the aircraft would be decelerating. Clearly the engine exhaust plumes contribute to the integral at the outflow plane, but there is no explicit separation of aerodynamics and propulsion in the formulation.

The momentum balance in figure 2 is written for a right handed coordinate system x, y, z defined by x in the flight direction, z towards the centre of the earth and y to starboard. Velocities along x, y and z are u, v, and w respectively. The energy balance is;

$$\int \rho u (h + 0.5(u^2 + v^2 + w^2))\, dA = \rho_\infty u_\infty (h_\infty + 0.5 u_\infty^2) A + \dot{m}_f h_f \qquad (3.1)$$

where: h is the enthalpy and the subscript f refers to the fuel while ∞ refers to the free stream. Note that at a given velocity u_∞ optimising cruise performance can be simply expressed as minimising the fuel mass flow m_f while supporting the aircraft weight.

There are a number of design guides made apparent by this CV:

1. a vertical velocity, w, must exist in the wake;

2. to minimise the vertical kinetic energy, w should be small and hence the aircraft should interact with the biggest airmass possible in order to support its weight;

3. sideways velocity v appears only in the energy balance and should be kept to an absolute minimum and hence aircraft volume should be accommodated by deflecting the air downwards and not sideways;

4. the wake should be uniform, as a region with low w must be compensated by higher w elsewhere. Since kinetic energy is proportional to w^2 the total kinetic energy is always higher in the non-uniform wake;

5. the enthalpy in the wake should be minimised and hence the wake should be as cold as the second law allows;

A caret wing wave rider immediately suggests itself as an ideal form as it is cut from a wedge flowfield and hence satisfies both conditions 3 and 4. Note that wave riders derived from axisymmetric flowfields such as those over a cone, create v in the wake and therefore will not be as efficient. However a caret wing does not interact with the maximum possible airmass and hence doesn't satisfy condition 2 as it leaves the flow over the top of the wing unperturbed. This is the reason waveriders are not competitive at low Mach number where it is generally recognised that expansion of the flow over the top of the wing will make a significant contribution to the lift. Less well recognised is that even hypersonic aircraft benefit significantly from expanding the lee flow. It will be shown below how this might be implemented in practice.

When considering condition 2 it should be remembered that the aircraft is interacting with an airmass defined by the intersection of the envelope of forward swept Mach lines from its trailing edge, with the shock/sonic waves from its leading edge. That is, the *interactive* airmass is not the same as the *perturbed* airmass shown in the control volume drawn in figure 2. Clearly the perturbed airmass increases with increasing distance to the chosen outflow plane, but the interactive airmass is not a function of control volume definition.

3.2 The two stream solution

Once it is accepted that expansion in the lee will be part of the optimum solution (to maximise airmass, condition 2) then it is apparent that there will be a compromise between conditions 2 and 4, since compression of the windward flow and expansion of the leeward flow will result in two states within the wake. Uniformity (condition 4) still holds true for both leeward and windward streams, thus for optimum efficiency the compromise mentioned can be interpreted as the optimum balance of the two mass flows and their separate uniform states.

Up to this point, the propulsive stream has been implicit in the stream thrust and energy balances, but has not been identified in the wake. In a conventional design like the XB-70 the propulsive stream would appear as narrow high velocity jets of hot exhaust gas. The minimum static enthalpy of the exhaust plumes is determined by the entropy increase within the engine and its associated flowpath (intake and nozzle). Although one might now expect a third uniform stream to be included in the analysis, it will be shown below that high cruise efficiencies are predicted if the leeward flow is composed entirely of exhaust flow.

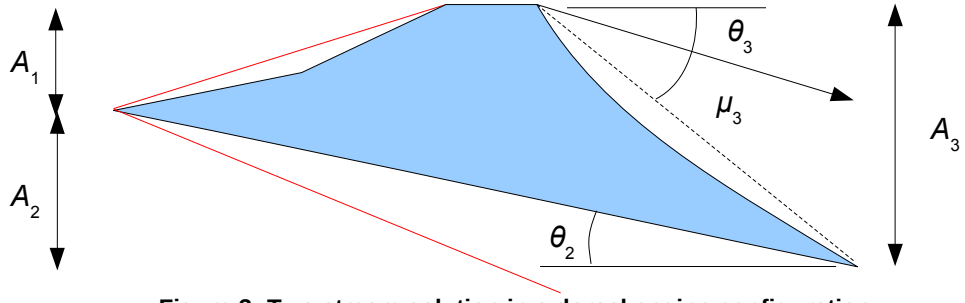

Figure 3: Two stream solution in a dorsal engine configuration

For this analysis, areas and angles are as defined in figure 3. Subscript 1, 2 and 3 refer respectively to: the captured propulsive flow at free stream conditions; the compressed lifting flow; and the engine exhaust. The exhaust is directed downward at θ_3, turning the lee airflow through the same angle and resulting in a pressure p_3 that is lower than ambient and determined by the Prandtl-Meyer equation. The exhaust Mach line is a straight connection between the cowl and base trailing edges at Mach angle μ_3 relative to the parallel streamlines in the uniform exhaust at pressure p_3.

The control volume is defined by tracing along the shock wave from the leading edge, over the top surface, down the exhaust Mach line, and then back to the leading edge along the bottom surface. Mass, momentum and energy balances allow the direct calculation of cruise efficiency, defined here as,

$$\eta_c = \eta_p \frac{L}{D} = \frac{T u_\infty}{\dot{m}_f h_f} \frac{L}{D} = \frac{L u_\infty}{\dot{m}_f h_f} \tag{3.2}$$

The lift L is the net vertical force on the CV and it is related to the fuel mass flow through the geometry of figure 3 and by the requirement that there be no net horizontal force.

3.3 Application to a supersonic transport

This CV approach to cruise performance optimisation was developed within the EU FP6 ATLLAS project and applied to the conceptual design of a Mach 3.5 transport aircraft. The result is depicted in figure 4. The central feature of the concept is a wide body 6.8m diameter fuselage sheltered behind a nose mounted variable geometry mixed compression intake. A high bypass turbofan within the nose acts as a compressor at flight Mach numbers below 2.5, feeding a transfer duct which moves air rearwards below the 40m cabin to ramjet combustors buried in the wing and tail. The turbofan/compressor does not operate at Mach numbers above 2.5 and all the fuel is burnt in the combustors within the aircraft tail and wings. The two

wing pods have a similar arrangement to the fuselage, but with fuel tanks rather than a cabin above the transfer duct. The single nozzle along the wing trailing edge, highlighted in blue, was stream traced from a 2D MOC flowfield.

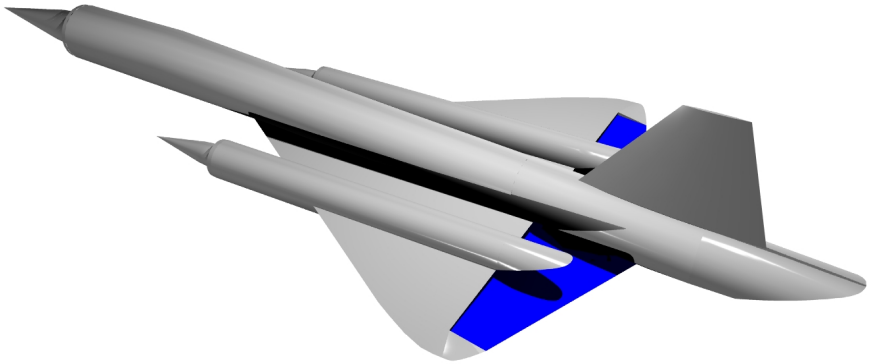

Figure 4: The ATLLAS M3T. An example of a highly integrated propulsion/ airframe concept

To relate this 3D concept to the 2D sketch in figure 3, it should be noted that the intake areas sum to A_1, the wing area is $A_2/\tan(\theta_2)$ and $A_3=A_1+A_2$ corresponds to the sum of the wing, fuselage and nacelle base areas (the total exhaust area). For maximum cruise efficiency the drag due to lift of the lifting stream is equal to the zero lift drag, and using linear theory for the pressure p_2,

$$\theta_2^2 = \frac{C_{D0}}{2}\sqrt{M_1^2 - 1} \tag{3.3}$$

where C_{D0} is the zero lift drag coefficient based on wing area. The zero lift drag is primarily the result of skin friction although other forms of parasitic drag such as that due to blunted leading edges may be included. Note from figure 3 that there is no drag due to thickness (volume) or base. Wing volume was created by downward deflection of the lifting stream, fuselage and nacelle volume by capturing the propulsive stream. Base area is (almost) completely occupied by the exhaust. The inevitable small departures from this ideal picture may be accounted for within C_{D0}.

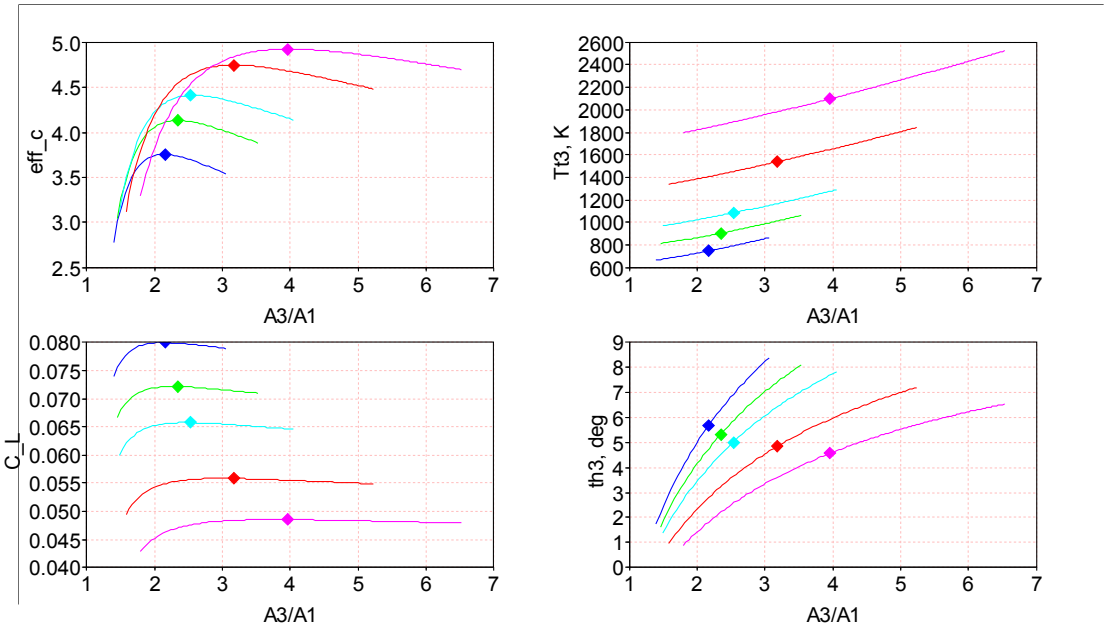

Figure 5: The effect of base to capture area ratio on cruise efficiency, total lift coefficient, exhaust total temperature, and thrust vector angle. Flight Mach numbers of 3, 3.5, 4, 5 and 6 correspond to blue, green, cyan, red and pink respectively.

Calculated results for aircraft cruising at Mach 3 to 6 are presented in figure 5 with an assumed intake pressure recovery following MIL-E-5007D,

$$P_{ti}/P_{t1}=1-0.075\left(M_1-1\right)^{1.35} \tag{3.4}$$

Pressure drop in the transfer duct and across the combustor is taken as P_{t3}/P_{ti}=0.9. The top left plot of figure 4 shows that cruise efficiency has a maximum at a particular value of A_3/A_1, for each Mach number. The other parameters, such as exhaust total temperature and deflection angle that are associated with this optimum area ratio are marked with symbols. Of particular interest are the relatively low exhaust total temperatures below Mach 4, and that the optimal exhaust deflection is approximately 5° irrespective of flight Mach number.

3.4 Scramjet examples

The relevance of the previous section to this lecture on scramjet nozzles is to suggest that the definition of the nozzle should be part of the overall aircraft design. In fact within the EU FP7 LAPCAT-2 programme we at GDL attempted to do just that, extending the optimisation procedure to Mach 8 with a reasonable fidelity scramjet intake/combustor/nozzle model. Cruise efficiencies of 3.9 were predicted but the very long nozzles associated with expansion to pressures below ambient proved entirely incompatible with any 3D implementation of the ideal 2D flow field, of which we could conceive. We were left with insufficient volume and clear indications of excessive structural mass.

Nozzle optimisation for the Dual Fuel cruiser [3-5], a ventral (under-slung) engine configuration on which the X-43A was based [6], involved a parametric study of the effect of length and expansion ratio on cruise efficiency. That is, the engine and the bulk of the airframe were fixed and two parameters that define the nozzle were allowed to vary. Significantly it was cruise efficiency rather than say axial thrust which determined the optimum, but such a procedure still accepts the risk that better cruise efficiency might be found with a completely different ratio of propulsive to lifting flows. At least the limitations to the design space imposed by the McDonnell-Douglas/NASA team guaranteed a realisable configuration.

4 THRUST-OPTIMISED LENGTH-CONSTRAINED NOZZLES

4.1 Rocket nozzle relevance

Rocket launcher payload fractions are very sensitive to both specific-impulse, I_{sp}, and structural mass. Since the optimum nozzle is the one that results in the highest payload fraction, these two parameters both figure in the optimisation of the nozzle contour. The methods developed for that purpose are therefore relevant to scramjet-powered aircraft or launcher concepts which are marginal at best, and hence just as sensitive to I_{sp} and mass. The design problem can be expressed as maximising thrust for a given mass flow (the ratio defining I_{sp}) in a given length nozzle (an indicator of structural mass). Guderley and Hantsch [7] solved the problem using the Lagrange multiplier method by which a maximum of a multi dimensional function is found when the function is subject to a number of constraints. Their mathematics was simplified by Rao [8], and such thrust optimised nozzles are sometimes called Rao nozzles. When applied to scramjet nozzle design, one could consider this to be the second step in the process. Having found the optimum propulsive mass flow and thrust vector angle, application of Rao's method may lead to higher payload fractions by reducing nozzle length and mass, accepting a reduction in exhaust uniformity.

4.2 Rao's method

Rao's simplification to the Guderley and Hantsch method for axisymmetric nozzles involved introducing an additional degree of freedom by not specifying that the CV surface on which thrust and mass flow would be determined, is defined by the Mach line that intersects the nozzle lip. Instead, the surface that intersected the lip was allowed to vary in angle relative to the axis as an unspecified function of radius, to be determined as a result of the optimisation. Intriguingly introducing this additional unknown, simplified the problem despite the fact that two results of the procedure are: first the resulting control surface is a Mach line; and second, and necessarily so, the compatibility relation is not violated along the line.

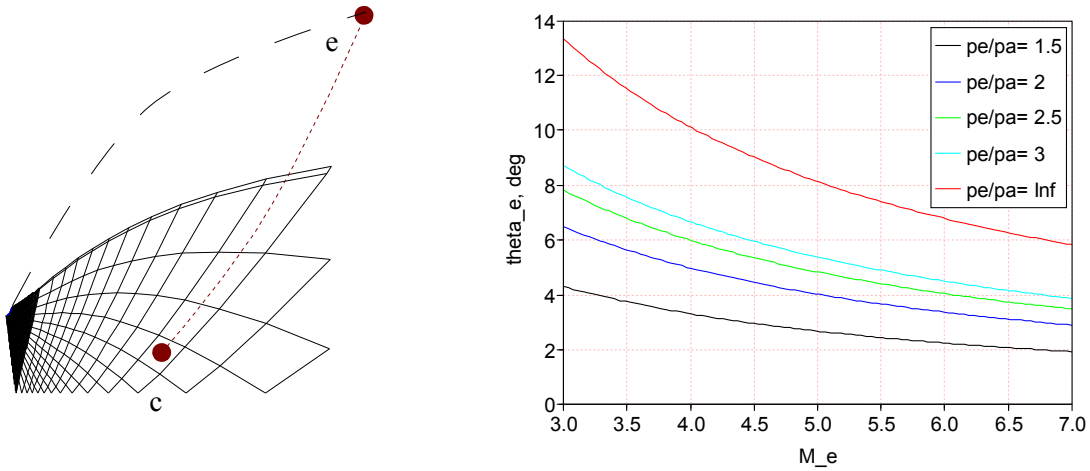

Figure 6: The MOC kernel and control surface *c-e*. On the right: the streamline angle at the lip for maximum thrust as a function of local exhaust pressure and Mach number.

Figure 6 illustrates Rao's approach. The characteristic mesh is generated by an expansion from the transonic solution at the throat, with the initial expansion rate being set by a predefined radius of curvature. The characteristics are Mach lines within the flow, running both to the left and right of a streamline at the local Mach angle. The right runners are directed inwards, towards the centreline, in this solution and the left runners are propagating outwards. The compatibility relations that hold at the intersection of the left and right runners enable the flowfield to be defined in a stepwise process. For scramjet applications the upstream data line could be obtained from a known combustor exit profile, rather than the transonic solution, with the subsequent steps in the method unaltered. However it is necessary

that the profile be approximated with constant stagnation enthalpy and entropy, which is an issue discussed later.

Rao's method addresses the problem of defining Mach number, M, and streamline angle, θ along the control surface drawn connecting c to e in the figure. The point e is at the nozzle lip but is undefined in x and y, the axial and radial coordinates respectively. Point c lies somewhere within the mesh generated by the initial expansion (the kernel). All that can be said about point c is that once its position has been determined, all other parameters there are known. That is, M_c, θ_c the mass flow passing through the right running characteristic that connects it to the wall, and the axial stream thrust between it and the centreline are all known from the kernel. Rao applied the method of Lagrange multipliers (see wikipedia.org for a general description) and determined that c and e are connected by a left running characteristic, and that along this characteristic,

$$\frac{w\cos(\theta-\mu)}{\cos\mu}=-\lambda_2 \tag{4.1}$$

and,

$$y\rho w^2\sin^2\theta\tan\mu=-\lambda_3 \tag{4.2}$$

λ_2 and λ_3 are constants (the Lagrange multipliers) and considering λ_2 if the velocity w is known and hence also the Mach angle μ (from the stagnation enthalpy), then the streamline angle, θ may be calculated from λ_2. Since the density, ρ, is also known for the expansion to w, the radius y can be calculated from λ_3. The last output of the method provides the relationship between w and θ at the lip, point e, and thus allows the calculation of λ_2. This is,

$$\frac{1}{2}\rho_e w_e^2\sin 2\theta_e \;=\; (p_e-p_a)\cot\mu_e \tag{4.3}$$

where p_e is the pressure after expansion to w_e and p_a is the ambient pressure. The radius at the lip y_e, and hence λ_3 are determined by finding the locus of points within the kernel that are compatible with λ_2 and then finding point c along this locus by ensuring the mass flow between c and e, matches the mass flow known from the kernel. This step involves the simultaneous solution of y_e, and y_c that can be achieved by numerical interpolation.

Streamline angle at the lip, θ_e, is plotted as a function of p_e/p_a assuming a constant ratio of specific heats γ=1.4 in figure 6. Note that this γ is only relevant to the relationship between p/ρ and the speed of sound along the characteristic c to e and has nothing to do with the high temperature properties of the reacting flow upstream in the nozzle. Thus a constant ratio of specific heats that corresponds to frozen chemistry and frozen vibrational excitation may be perfectly adequate and certainly far better than the common practice of applying a meaningless 'high temperature gamma' to the nozzle exit flow. The subsequent calculation of the nozzle contour by MOC applied between the right running characteristic to c in the kernel, and the left running characteristic from c to e, is a separate problem that requires a non-equilibrium MOC technique such as that presented in section 5.

I think it is important to reiterate that the output of Rao's method is not a nozzle contour but the definition of flow properties along the final characteristic which will result in maximum thrust for a given p_e/p_a. Increasing values of this ratio correspond to decreasing nozzle length, and with Rao's method at each length the maximum thrust is guaranteed. With p_e/p_a=1 the optimum distribution is parallel uniform flow, like a wind tunnel nozzle, and the absolute maximum in inviscid thrust is obtained. Once the inviscid contour is found, one can calculate the friction force and by subtraction, find that the maximum obtainable thrust which will inevitably occur with p_e/p_a>1. Maximum payload or maximum range is likely to occur

with even higher values of p_e/p_a and thus the optimum for the application will depend on the sensitivity to I_{sp} and mass.

4.3 Stream traced nozzles

Direct application of a thrust optimised axisymmetric nozzle would be problematic for many hypersonic aircraft concepts like the X-43 but less so for hypersonic missiles with geometry such as Hyfly or the X-51. Greater adaptability is provided by using the stream tracing technique introduced by Evvard and Maslen [9] which allows nozzles of arbitrary cross sections to be derived by tracing the streamlines that coincide with the perimeter of the cross section through a 'template' axisymmetric flowfield.

Conditions along the last characteristic of the thrust optimised template flowfield will not generally be given by equations 4.1 to 4.3, because those equations are derived assuming the full 2π arc at each radius contributes to the thrust and mass flow integrals. With stream tracing, the arc angle is a function of radius and direct application of Rao's method results in an optimum that is incompatible with the flow equations for the axisymmetric template. To prevent this an additional constraint has to be added, but the elegance of Rao's simplification is lost and no analytical solution has been found. The problem is the subject of ongoing research, but perhaps it is worth noting that the optimum we are seeking is a maximum in propulsive lift with constrained axial thrust, mass flow, and nozzle length. We may resort to a parametric trial-and-error approach, which then would allow the introduction of non-uniform stagnation enthalpy and entropy at the combustor exit, while simultaneously eliminating all the fun in the design.

5 A METHOD OF CHARACTERISTICS FOR NON-EQUILIBRIUM FLOWS

5.1 Introduction

Having determined the ideal propulsive flow from an approach such as that outlined in section 3 and then traded exhaust uniformity for nozzle mass using a technique such as that applied to rocket nozzles and described in section 4, it is then necessary to determine the contour that will produce the corresponding exhaust velocity distribution.

Typical scramjet combustor exit pressures and temperatures are such that the exhaust will be in chemical non-equilibrium, although not necessarily frozen. The generation of the MOC mesh for the kernel and the subsequent development of the contour once the exit characteristic is established, requires a MOC applicable to non-equilibrium reacting flows. Development of such a code can be rather daunting with significant numerical obstacles imposed by the wide variation in chemical and flow time scales. In this section a simple and accurate method is described. It is presented in sufficient detail to be understood and followed as it has not been published previously.

5.2 The compatibility equation

The physical significance of Mach number is most apparent when it is defined by [10],

$$M^2 = -\frac{d\rho}{\rho}\frac{w}{dw} \tag{5.1}$$

The dimensionless group is then recognisable as a balance of two competing processes within a compressible flow: density dilation and velocity deformation. At very low Mach number fluid elements experience little change in density and elongate as they accelerate through an area restriction. Conversely at very high Mach number, velocity changes are small and the fluid compresses or expands to accommodate changes in stream tube area. Within a two or three dimensional flow, the density and velocity derivatives that determine/exhibit this balance are those along streamlines.

Consider axisymmetric inviscid flow in cylindrical coordinates with x being the axial direction and y the radius. The angle of a streamline relative to x is denoted θ. Working first in natural coordinates, and using the suffixes z and n to indicate derivatives taken along, and normal to, the streamline respectively, the continuity equation is,

$$\theta_n + \frac{w_z}{w} + \frac{\rho_z}{\rho} = \theta_n + \frac{w_z}{w}\left(1 - M^2\right) = -\frac{\sin\theta}{y} \tag{5.2}$$

The velocity w is along the curvilinear coordinate z aligned locally with the streamline. The momentum balances along and normal to the streamlines are respectively,

$$w\, w_z + p_z/\rho = 0 \tag{5.3}$$

$$\theta_z + p_n/(\rho\, w^2) = 0 \tag{5.4}$$

The directions within the flow set by

$$\frac{dz}{dn} = \pm\beta = \pm\sqrt{M^2 - 1} \tag{5.5}$$

have particular significance to the solution of these equations. Denoting a derivative in either of these directions by the superscript ', and noting that,

$$\theta' = (\theta_n \pm \beta\,\theta_z)\,n' \text{ and } p' = (p_n \pm \beta\, p_z)\,n' \tag{5.6}$$

equations 5.2 to 5.4 may be reduced to,

$$\pm\theta' + \frac{\beta\, p'}{\rho\, w^2} + \frac{\sin\theta}{y\sqrt{\beta^2 + 1}} = 0 \tag{5.7}$$

The above equation appears to be the compatibility equation along characteristics defined by equation (5.5), and in some important practical cases β, as defined, does set the characteristic direction. Unfortunately when Resler [11-13] presented a similar analysis fifty years ago, he did not define the limits to application and his publications proved to be controversial. The counter arguments that were raised [14-16] and the consensus/textbook [17] view on the subject are discussed while demonstrating the utility of equation 5.7.

5.3 Resler's sound speed in reacting flow

Substitution of equation 5.3 into 5.1,

$$M^2 = w^2\left(\frac{\partial\rho}{\partial p}\right)_n = \left(\frac{w}{a}\right)^2 \tag{5.8}$$

The sound speed, a, first defined this way by Resler [11] assumes the usual values in frozen and equilibrium flows since in these cases entropy is constant along streamlines and therefore the derivative along z (constant n) is identical to the derivative at constant entropy.

Within a reacting flow, sound speed is known to be a function of frequency. When the wave period is much shorter than the reaction time-scale, the wave travels at the frozen (non-reacting) sound speed and conversely when the period is very long in comparison, the wave travels at the equilibrium sound speed.

The fact that at intermediate frequencies waves dissipate and spread [14, 15] is a reflection of the fact that the density and pressure gradients within the wave are intimately coupled with the wave speed through conservation of mass and momentum in precisely the manner made apparent by equations 5.2 and 5.3.

Within a steady flow, local property gradients do not vary with time but in general will vary with direction. Since β is defined by a gradient along streamlines and yet is present in equation 5.7, the equation is not an ordinary differential equation unless Resler's speed of sound happens to be a property of the fluid. This is the case when entropy is constant along streamlines, as mentioned previously, but also when a reacting gas undergoes very similar rates of expansion along all stream tubes. In the latter case the entropy need not be constant but since p will have a unique relationship with ρ the derivative that defines Resler's speed of sound becomes independent of direction, and equation 5.7 is then a compatibility equation.

Apart from its practical application, Resler's speed of sound and associated characteristic direction provides a philosophical bridge between the frozen and equilibrium characteristics. The idea that the characteristic direction makes an instantaneous transition from frozen to equilibrium at the moment the flow reaches equilibrium [17], does not help explain why the equilibrium characteristics are relevant to any flow, since there must always be a small departure from equilibrium to drive the state changes. On that basis one should expect the characteristic direction to always be set by the speed of sound with every internal energy mode frozen, not only chemical but also the electronic, vibrational, and rotational states. Adopting Resler's approach, transition to equilibrium characteristics is a gradual process occurring as the rate of change becomes sufficiently low that it does not affect the way pressure varies with density.

5.4 Loosely coupled solution

Integration of equation 5.7 is straightforward when there is a unique relationship between the variables p, ρ and w (and hence also β via equations 5.5 and 5.7) The flow field calculation may be greatly simplified by direct integration (and tabulation) of the second term in equation 5.7 prior to the generation of the characteristic mesh.

For the general case of a reacting ideal mixture of ideal gases, the task is perhaps clearest when the equation of state, $p=\rho RT$, where R is the mixture's gas constant, is used to recast equation 5.7 into the form,

$$\pm\theta' + \frac{\beta RT}{w^{-2}}(\ln p)' + \frac{\sin\theta}{y\sqrt{\beta^2+1}} = 0 \qquad (5.9)$$

The usual finite difference technique can be applied provided one has tables of the generally slowly-varying integrand and ln(p) for the three streamlines bridged by the characteristics. These are the streamlines at the origin of the left and right running characteristics and the streamline at their intersection. The problem is split into two weakly coupled parts: The fluid dynamic problem of solving the momentum and continuity equations for pressure and streamline angle using MOC; and the thermodynamic and chemical kinetic problem of establishing the state of the gas along streamlines. The appropriate start to the solution is problem dependent, but in general one makes some approximation for the gas state development, computes the flowfield and then records how the calculated rate of change of temperature (dT/dt) varies with temperature, T, along streamlines. This relationship is then applied in a second thermodynamic calculation of the gas state to improve the approximate relationship between the integrand and ln(p), before recomputing the flowfield. Two or three iterations may be required.

5.5 Energy and chemistry along streamlines

The thermodynamic properties of an ideal mixture of ideal gases can be determined from the molar concentrations c_i of its constituent species (index i) and its temperature. Therefore the thermodynamic aspect of the non-equilibrium flowfield solution may be simply stated as; find c_i as a function of T along particular streamlines, given dT/dt computed by MOC.

Noting specific stagnation enthalpy (J/kg) does not vary along a streamline, the differential form of the first law for this steady-state system may be written,

$$\sum c_i dh_i + \sum h_i (d c_i)_v + \rho w dw = 0 \tag{5.10}$$

where h_i is the species molar enthalpy (J/mol) including the enthalpy of formation. The subscript v refers to concentration changes that result from chemical reactions at constant volume. The total change in concentration of species i is,

$$dc_i = (d c_i)_v + c_i d\rho / \rho \tag{5.11}$$

The chemical changes are calculated from an appropriate chemical kinetic scheme and an example is given in the following section.

Combination of equation 5.10 with the z momentum equation 5.3, provides an expression for the stream wise change in pressure,

$$dp = \sum c_i dh_i + \sum h_i (d c_i)_v \tag{5.12}$$

Summing equation 5.11 over all species and combining with the ideal gas equation of state provides an expression for the density change,

$$\frac{d\rho}{\rho} = \frac{dp}{p} - \frac{dT}{T} - \frac{\sum (d c_i)_v}{\sum c_i} \tag{5.13}$$

which after substitution back into equation 5.11, allows species concentrations to be found by numerical integration. Here we used the accurate and stable Scilab function ODE (www.scilab.org). For convenience, temperature was used as the independent variable by application of the chain rule,

$$\frac{d c_i}{dT} = \frac{dc_i}{dt}\frac{dt}{dT} \tag{5.14}$$

Resler's sound speed is obtained directly from the differentials for p and ρ (equations 5.12 and 5.13).

5.6 Fuel/Air chemistry

The temporal rate of change of concentrations at constant volume are found from,

$$\left(\frac{\partial c}{\partial t}\right)_v = N\dot{J}, \quad \dot{J}_j = kf_j \prod c_i^{N_{ij}^-} - kr_j \prod c_i^{N_{ij}^+} \tag{5.15}$$

N is the matrix of stoichiometric coefficients defining the reaction scheme, with those species involved in the forward reaction given negative values; $\dot{J}$ is the vector of reaction rates with element j defined

above, note the separation of the positive and negative values of N; kf_j and kr_f are the forward and reverse reaction rates respectively.

The forward rate constant are normally calculated from empirical correlations in the form,

$$kf_j = B_j A_j T^{n_j} \exp(-T_j / T) \tag{5.16}$$

where A_j, n_j, and T_j (the activation temperature of reaction j) are constants defined by the reaction mechanism, and B_j=1 unless a third body molecule is involved, in which case, $B_j = \sum_i \epsilon_{ij} c_i$ where ε_{ij} is the third body efficiency of species i in reaction j.

The reverse rate is calculated from the forward rate and the equilibrium constant, K_j,

$$kr_j = \frac{kf_j}{K_j}\left(\frac{\bar{R}T}{p^0}\right)^{\sum_i Nij} \qquad K_j = \exp\left(\frac{-\Delta G^0}{\bar{R}T}\right) \tag{5.17}$$

with K_j calculated from the change in Gibbs free energy, ΔG^0, at the reference pressure, p^0=10^{5}Pa. $\bar{R}$ is the universal gas constant in J/mol/K and all thermodynamic properties of the individual species can be calculated from polynomials for specific heat such as those provided in the thermo.inp file of CEA [18].

5.7 Frozen characteristics

The established characteristic direction within a non-equilibrium flow is that set by Mach number based on the frozen speed of sound, M_f. The compatibility relations may be obtained by substitution of w_z from equation 5.2 into equation 5.1 and adding to the multiple of equation 5.4 and β_f resulting in,

$$\theta_n + \beta_f \theta_z + \frac{\beta_f p_n - p_z}{\rho w^2} + \frac{\rho_z}{\rho} = -\frac{\sin\theta}{y} \tag{5.18}$$

The density derivative along the streamline is found from equation 5.13 with the temperature derivative obtained from equation 5.12 by recognising $dh_i = C_{pi}\, dT$. The result is,

$$\frac{d\rho}{\rho} = \frac{dp}{p} - \frac{dp - \sum h_i (dc_i)_v}{T \sum c_i C_{pi}} - \frac{\sum (dc_i)_v}{\sum c_i} \tag{5.19}$$

Now since,

$$\rho w^2 = \rho M_f^2 \gamma_f RT = \gamma_f p(\beta_f^2 + 1) \tag{5.20}$$

where γ_f is the ratio of specific heats with locally frozen chemistry. Substitution of equation 5.19 into 5.18 provides the compatibility relations,

$$\pm\theta' + \frac{\beta_f p'}{\rho w^2} + \frac{\sin\theta}{M_f y} = \frac{\sum h_i (\partial c_i / \partial z)_v}{M_f T \sum c_i C_{pi}} + \frac{\sum (\partial c_i / \partial z)_v}{M_f \sum c_i} \tag{5.21}$$

Note that the partial derivatives on the right hand side are direct functions of the local state (not gradients in state) in the manner outlined in the section on chemistry and therefore, unlike equation 5.7, this equation is always an ordinary differential equation. That is, β_f is always a characteristic direction, even within an equilibrium flow, but clearly in that case there is more than one characteristic direction.

Having shown that β is also a characteristic direction in restricted cases, the choice of what direction to take in an application of MOC is a question of which allows the most direct and accurate solution. At a time when CFD flow field solutions locked to geometric grids and coordinates are common, there may be less resistance to the application of equation 5.7 than Resler encountered, even in the case where the relationship between density and pressure varies from streamline to streamline and β is not strictly a characteristic direction. However there are some supersonic flow fields within which β is complex and hence undefined just as it is in subsonic flow.

6 CONCLUSIONS

- The aim of nozzle design is to maximise the increase in stream thrust between that at the nozzle throat and that at the nozzle exit.
- Prior to contour design it is necessary to determine the optimum exit area and thrust vector orientation under constraints imposed by the vehicle and its mission. The propulsive stream thrust is likely to make a substantial contribution to lift and moments. Choice of an appropriate control volume simplifies this task.
- Rao's method provides a means to maximise nozzle thrust when constrained by length.
- Stream tracing allows complex 3D geometry to be obtained from 2D (or 1D) template flowfields, if required for better vehicle integration.
- MOC enables the contour to be developed for reacting, non-equilibrium expansions, and is simplified by taking Resler's characteristic direction.

7 REFERENCES

[1] STAFF AT JHU-APL, 1964, *Handbook of supersonic aerodynamics, section 17: Ducts, nozzles and diffusers*, NAVWEPS report 1488, Vol. 6, available from DTIC as AD613055;

[2] VAHL W., and WEIDNER J., 1980, *A preliminary assessment of the effect of 2-D exhaust-nozzle geometry on the cruise range of a hypersonic aircraft with top-mounted ramjet propulsion*, NASA-TM-81841;

[3] BOGAR T., EISWIRTH, COUCH L., HUNT J., and McCLINTON C., 1996, *Conceptual design of a Mach 10, global reach reconnaissance aircraft*, AIAA-1996-2894;

[4] BOGAR T., ALBERICO J., JOHNSON D., ESPINOSA A., and LOCKWOOD M., 1996, *Dual-fuel lifting body configuration development*, AIAA-1996-4592;

[5] WEIRICH T., FOGARTY W., DRY K., IQBAL A., and MOSES P, 1996, *Dual-fuel airframe and engine structural integration*, AIAA-1996-4594;

[6] ENGELUND W., HOLLAND S., COCKRELL C., and BITTNER R., 1999, *Propulsion System Airframe Integration Issues and Aerodynamic Database Development for the Hyper-X Flight Research Vehicle*, ISOABE-99-7215;

[7] GUDERLEY G., and HANTSCH E., 1955, *Beste Formen fur Achsensymmetrische Uberschallschubdusen*, Zeitschrift fur Flugwissenschaften, Brauschweig;

[8] RAO G., 1958, *Exhaust Nozzle Contour for Optimum Thrust*, Jet Propulsion 28, pp. 377-382;

[9] EVVARD J., and MASLEN S., 1952, *Three-Dimensional Supersonic Nozzles and Inlets of Arbitrary Exit Cross Section*, NACA-TN-2688;

[10] STALKER R., 1980, *Lectures in gas dynamics*, Mechanical Engineering, University of Queensland;

[11] RESLER E., 1956, *Sound speed in a reacting medium*, J. Chem. Phys., Vol. 25, pp1287-1288;

[12] RESLER E., 1957, *Sound speed*, J. Chem. Phys., Vol. 27, pp596-597;

[13] RESLER E., 1957, *Characteristics and sound speed in nonisentropic gas flows with nonequilibrium thermodynamic states*, J. Aeronaut. Sci., Vol. 24, pp785-790;

[14] WOOD W. and KIRKWOOD J., 1957, *Characteristic equations for reactive flow*, J. Chem. Phys., Vol. 27, pp596;

[15] BROER L., 1958, *Characteristics of the equations of motion of a reacting gas*, J. Fluid Mech., Vol. 4, pp276-282;

[16] EHLERS F., 1963, *Method of characteristics and velocity of sound for reacting gases*, Vol. 1, No. 6, pp1415-1416;

[17] HAYES W. and PROBSTEIN R., 2003, *Hypersonic inviscid flow*, Dover Publications, NY, p539;

[18] GORDON S., and McBRIDE B., 1994, *Computer program for calculation of complex chemical equilibrium compositions and applications*, NASA-RP-1311;